JMSA ISSN: 1079-8501

Vol. 1 No. 6: pp. 267-279, 1995

Design and Initial Performance of an Ultrahigh Vacuum Sample Preparation Evaluation Analysis and Reaction (SPEAR) System

C. Collazo-Davila,[1] E. Landree,[1] D. Grozea,[1] G. Jayaram,[1]
R. Plass,[1] P. C. Stair,[2] and L. D. Marks[1]
[1]*Department of Materials Science and Engineering, Northwestern University, Evanston, Illinois 60208;*
[2]*Department of Chemistry, Northwestern University, Evanston, Illinois 60208*

Abstract: Results concerning the calibration and use of a new ultrahigh vacuum (UHV) surface preparation and analysis system are reported. This Sample Preparation Evaluation Analysis and Reaction (SPEAR) side chamber system replaces an older surface side chamber that was attached to a Hitachi UHV H-9000 microscope. The system combines the ability to prepare clean surfaces using sample heating, cooling, ion milling, or thin film growth with surface analytical tools such as Auger electron spectroscopy (AES), X-ray photoelectron spectroscopy (XPS), and scanning electron microscopy (SEM), along with atomic surface structure information available from high-resolution transmission electron microscopy (HREM). The chemical sensitivity of the XPS and AES are demonstrated in preliminary studies of catalytic and semiconductor samples. In addition, the surface preparation capabilities are also demonstrated for the Si(100) and Ge(100) surfaces, including the ability to acquire secondary electron images during milling. During operation, the entire system is capable of maintaining the UHV conditions necessary for surface studies.

Key Words: ultrahigh vacuum (UHV), transmission electron microscopy (TEM), surface science, surface analytical techniques.

1. Introduction

Atoms in the surface region of a crystal exist in a different environment than those in the bulk. Small shifts in the atom positions from the "normal" bulk lattice sites can result in a net lowering of the total energy of the system. In a clean surface layer kept under ultrahigh vacuum conditions, a structural rearrangement of the surface atoms such as a "relaxation" or a "reconstruction" can occur. Over the last several decades many different methods have been developed for probing these surface structures. While scanning tunneling microscopy (STM) and atomic force microscopy (AFM) have provided a wealth of knowledge about surfaces on the atomic level (Rohrer, 1994), they suffer from an important limitation: they are sensitive to only the outermost layer of atoms, and it has been suggested that surface reconstructions can involve relaxation of the top several layers of atoms near the surface extending into the bulk (LaFemina, 1992; Jayaram et al., 1993).

Two additional techniques that have been used to obtain surface information are scanning electron microscopy (SEM) and scanning transmission microscopy (STEM) (Venables et al., 1987; Milne et al., 1993; Endo and Ino, 1993). One particular advantage of these techniques is the numerous signals generated during operation which are capable of providing a great deal of information. In addition, SEM can provide three-dimensional images that are easily interpretable in terms of surface morphology. One of the drawbacks of SEM is that it is unable to gain image information below the top most layer of atoms or below the top two to three layers in scanning Auger microscopy. In addition, current SEM technology is unable to compete with the resolution capabilities of other electron probe techniques such as transmission electron microscopy (TEM) or STM. Even though STEM provides both surface and bulk information, the deconvolution of the two is not a straightforward process. Typically, STEM is operated using an annular dark-field detector to provide a two-dimensional potential projection of the thin film. Surface information from STEM must be obtained through a combination of imaging and other low energy electron signals such as Auger or secondary electrons. Such signals only allow resolutions on the order of nanometers due to electron scattering within the sample.

* Corresponding author: Christopher Collazo-Davila, Department of Materials Science and Engineering, Northwestern University, 2225 North Campus Drive 2036 MLSF, Evanston, IL 60208

Reflection electron microscopy (REM) is another well-understood technique that has been applied to the study of dynamic surface phenomena. However, the resolution of REM is limited by geometrically induced distortions caused by the grazing incidence of the electron beam with respect to the surface of the sample, resulting in an image that is foreshortened by a factor of 50 in the beam direction for flat surfaces (Nielsen and Cowley, 1976; Yagi, 1993).

Emission microscopes form a large group of related imaging techniques (Mundschau, 1991; Griffith and Engel, 1991). Included in this group are low-energy electron microscopy (LEEM); mirror electron microscopy (MEM), which is usually just one imaging mode of LEEM; and photo-electron microscopy (PEEM), which can be one of the imaging modes of a LEEM instrument (Bauer et al., 1989; Tromp and Reuter, 1993; Tromp, 1994) or a technique on its own. They all have in common an electric accelerating field present at the specimen surface, low-energy (100 eV) electrons for a gentle probing of the surface, and the requirement of relatively flat specimens. A direct imaging technique, LEEM provides surface sensitivity, large field of view, and high speed of image acquisition, but it lacks atomic resolution. In MEM the electron beam is reflected in front of the sample, which is the mirror surface, and it has to be combined with other surface techniques due to difficult interpretation. An ultraviolet, or other wavelength, light source is used in PEEM to eject photoelectrons; otherwise, the same specimen geometry and immersion lens are used. The magnification is often limited by emission current densities.

Over the past 20 years, several techniques have been developed for studying surface structures with the transmission electron microscope. Among the first to use transmission electron microscopy as a surface-sensitive tool was D. Cherns, whose work in the 1970s demonstrated the ability to resolve single atomic steps in a thin Au film (Cherns, 1974). Using bulk-forbidden reflections in the (111) Au diffraction pattern to form dark-field images, he was able to resolve contours whose intensity variation matched those predicted by theory to be single atomic steps. Plan-view HREM (Marks et al., 1992), profile HREM (Marks, 1983), and transmission electron diffraction (TED) (Takayanagi et al., 1985; Gibson, 1990; Marks et al., 1993; Jayaram et al., 1993; Jayaram et al., 1995) have been used successfully as a probe to characterize specific surface reconstructions. The advantage of TEM over many other techniques lies in its ability to provide information about the crystal structure extending into the bulk. TEM is also able to provide both real and reciprocal space information from the same region.

With the development of TEM as a powerful research tool for exploring surface structures, it is natural to apply the technique to important material issues such as thin-film nucleation and growth. Typical high-resolution transmission electron microscopes are able to gain structural information on the order of hundredths of a nanometer. However, in studying the initial stages of thin-film growth, TEM is limited by its lack of chemical information. Ideally, one would like to have the chemical binding information from either X-ray photoelectron spectroscopy (XPS) or Auger electron spectroscopy (AES) to complement the structural information available with TEM (Siegbahn et al., 1967; Briggs and Seah, 1983). With this marriage of structural and chemical information as motivation, our research group recently commissioned the design and construction of a surface preparation and analysis system. The **S**ample **P**reparation **E**valuation **A**nalysis and **R**eaction (SPEAR) system combines TEM, XPS, AES, scanning electron microscopy (SEM), a duoplasmatron ion gun for surface cleaning, and a molecular beam epitaxy (MBE) chamber for the study of surfaces, all under UHV conditions.

Our approach to surface studies is by no means unique; the following description of other UHV systems is intended to highlight the strengths and limitations of our own system (see also Table 1). Heinemann and Poppa (1986) discussed the addition of a UHV chamber between the condenser and objective lenses on a Siemens Elmiskop 101. Sample preparation techniques on the system include heating, oxygen/hydrogen plasma treatment, ion etching, and thin-film deposition from three wire evaporators. In a similar approach, the specimen chamber on a Jeol 2000EX microscope at the University of Illinois-Urbana was replaced with a full surface science chamber (Twesten et al., 1994). The modification to the optics limits the resolution to 3 nm, but the TEM capabilities are coupled with LEED, AES, a resistive specimen heater, and an evaporation source. Reflection electron microscopy (REM) and gas dosing are also possible. The system has produced some interesting results on oxidation and oxygen-etching of Si (Twesten et al., 1994). Kondo et al. (1991) have redesigned the optics, pumping system, and sample stages of a JEM-2000FX to allow UHV surface studies using REM and TEM. Evaporation sources, gas inlet equipment, and specimen heating stages are available for *in situ* investigations. Point to point resolution is 0.21 nm at 200 kV, and the microscope has a 2-nm electron probe size for chemical analysis and micro-area diffraction.

As an alternative approach, several groups have left the electron optics untouched. Although this preserves the resolution capabilities of the TEM, typically less peripheral equipment can be incorporated. Wilson and Petroff (1983) designed a cryoshroud for a JEOL 200B microscope, and the resulting vacuum at the sample allowed them to preserve reconstructed Si(111) and GaAs(100) surfaces for several hours. The microscope also had an evaporator and a sample heater. Metois et al. (1989) reported modifying a JEOL 100C ASID-4D by adding a cryoshroud and allowing a mild bake to reach UHV conditions. The system combined TEM, SEM, and REM with sample heating and evaporation sources. McCartney and Smith (1991) described a 300-kV Philips 430ST HREM modified for UHV opera-

TABLE 1

UHV Microscopes and Their Capabilities (Bonevich and Marks, 1992; Twesten et al., 1994)

Microscope	Vacuum and resolution	Characterization and preparation	Comments
JEOL 100B (Honjo et al., 1977)	2.7×10^{-7} Pa ≈ 0.35 nm	EBE, evap. ports and large tilting	Cryo and no side chamber
JEOL 2000CX (McDonald and Gibson, 1984)	1.3×10^{-7} Pa 0.25 nm	MBE, DRH, heating and cryogenic stage	Cryo and side chamber
Seimens/Elmiskop 101 (Heinemann and Poppa, 1986)	4×10^{-8} Pa ≈1.5 nm	MBE, OPC, SIG, heat/cryo stage, gas jet cleaning, evap.	Cryo and no side chamber environmental cell
JEM 2000FXV (Kondo et al., 1987)	2.7×10^{-7} Pa 0.21 nm	Six attachment ports, evap., heating stages, large tilt	No Cryo or side chamber
Hitachi UHV H-9000 (Marks et al., 1988)	**2.7×10^{-8} Pa 0.2 nm**	**LEED, AES, PEELS, SIG, IRH, OSA, laser, evap., ± 10° tilt**	**No Cryo, UHV transfer system**
Philips 430ST (Smith et al., 1989)	1.3×10^{-7} Pa 0.2 nm	Evap., SIG, heating stage, PIMS, ± 15° tilt	Cryo and prep. chamber
VG Microscopes (Hembree et al., 1989)	2.7×10^{-8} Pa ≈ 0.3 nm	AES, SED, SIG, MBE, PEELS, heating	Prep. chamber, 12 samples
JEOL 100C (Mètois et al., 1989)	8×10^{-7} Pa ≈ 0.7 nm	Evap., heating stage, STEM, REM, SED	Cryo, specimen air-lock
Philips EM430 (Bleeker, 1991)	1.3×10^{-8} Pa	PEELS, AES, evap., EDX, MBE, PIMS, ± 15° tilt	No Cryo and prep. chamber
JEM 2000FXV (Kondo et al., 1991)	2.7×10^{-7} Pa 0.21 nm	REM-PEEM, evap., heating stages, large tilt	Cryo and side chamber
JEOL 2000EX (Twesten et al., 1994)	Low 10^{-7} Pa 2.5 nm	LEED, AES, REM, heating stage, evap.	Cryo and replace specimen and objective region with surface science chamber
Hitachi UHV H-9000 and SPEAR	**2.6×10^{-9} Pa 0.2 nm**	**AES, XPS, SEM DRH, e-beam heating, PEELS, SIG, SIG images, SEM, MBE, SED, evap., ± 10° tilt**	**No Cryo, UHV transfer system (SPEAR), 18 samples**

Note: AES = Auger Electron spectroscopy; Cryo = cryopumping needed; DRH/IRH = direct/indirect resistive heating; e-beam heating = direct electron beam heating; EBE = electron beam evaporator; EDX = energy dispersive X-ray analysis; evap. = evaporation source; LEED = low-energy electron diffraction; MBE = molecular beam epitaxy; OPC = oxygen plasma cleaning; OSA = optical specimen annealing; PEELS = parallel electron energy loss spectroscopy; PIMS = precision ion mill system; SED = secondary electron detector; SEM = scanning electron microscopy; SIG = sputter ion gun.

tion. With the specimen holder heating the sample to 580°C, a resolution of 0.2 nm was reported. Our group's approach has been to leave the TEM optics intact and to place additional equipment in an adjoining chamber. The SPEAR system represents a second generation design for this approach, and it incorporates many improvements over our first microscope side chamber.

The previous UHV surface science chamber (SSC) (Dunn et al., 1991; Bonevich and Marks, 1992) was designed to perform *in situ* sample preparation of TEM specimens under UHV conditions and then transfer them to the microscope for structural analysis. The system included a sputter ion gun for surface cleaning, a high-current electron gun and high-intensity light source for sample annealing, and metal evaporation filaments. Although a productive instrument, the UHV-SSC did have several limitations. The original SSC system could only handle a single sample, which limited the number of workers who could use the system. In addition, it required 12 h to place a sample into the system, during which the microscope could not be used. The dependence of the microscope on the SSC resulted in inefficient use of equipment time.

Furthermore, the mechanism for manipulating the sample inside the SSC was limited and sometimes ineffective. A great deal of time was spent positioning the sample for preparation or transfer. None of these limitations could have been overcome easily by simply modifying the existing SSC. A new approach to the entire system was required and constitutes what is now the SPEAR system.

2. SPEAR System

2.1 Design Criteria

From the experience gained using the previous SSC, several fundamental criteria were adopted for the design of the new system. It was clear that in order for the microscope to be used most efficiently, a mechanism to transfer, store, and exchange multiple samples would be needed. The new system would also be designed with the ability to expand and adopt additional chambers, extending the lifetime of the system. Having a separate introduction chamber could avoid the down time experienced by the SSC during sample exchange, and a further improvement in efficiency could be realized by allowing electron microscopy, sample preparation/analysis, and sample exchange to operate independently of one another. The new system would also include an improved means of handling samples allowing them to move independently of the microscope cartridge. Precise control of the ion sputtering was another necessary feature to facilitate milling without the risk of inadvertently sputtering contaminants onto the surface of the sample. In addition, SPEAR would include the latest equipment for surface chemical characterization.

2.2 The SPEAR System

Figure 1 shows the Hitachi UHV H-9000 microscope (Marks et al., 1988; Marks et al., 1991; Bonevich and Marks, 1992) alongside the SPEAR side chamber system (Superior Vacuum Technology, Inc., now EPI, MBE Products Group, St. Paul, MN). The system, shown schematically in Figure 2, consists of four separate chambers, each with an individual task or function.

The load-lock chamber is used for introducing or retrieving samples from SPEAR. Up to five samples can be exchanged at a time through the load-lock without disturbing the vacuum conditions inside the rest of the system. Pumped by a 210 l/s turbomolecular pump (Balzers, Hudson, NH), the load-lock chamber is capable of going from atmospheric pressure to 1×10^{-8} Pa in 4 h. Once UHV is achieved, the load-lock can then be opened and the sample introduced into the transfer chamber.

The transfer chamber is pumped by a 400 l/s ion pump (Physical Electronics, Eden Prairie, MN), with a base pressure of 4×10^{-9} Pa. The transfer chamber consists of a storage module capable of holding up to eight samples and four microscope cartridges and a central transfer module used for shuttling samples between the various chambers. Through this chamber, a given sample may be transferred to any other part of the system or to the UHV microscope without breaking vacuum. In addition, an evaporation stage consisting of five different metal sources has been added to supplement the evaporators already present in the microscope. For future expansion there are three 4.5-in. ports and one 10-in. port to accommodate additional chambers or extensions.

The MBE chamber is pumped by a 220 l/s ion pump (Physical Electronics) and has a base pressure of 1×10^{-9} Pa. The chamber has been designed with four effusion

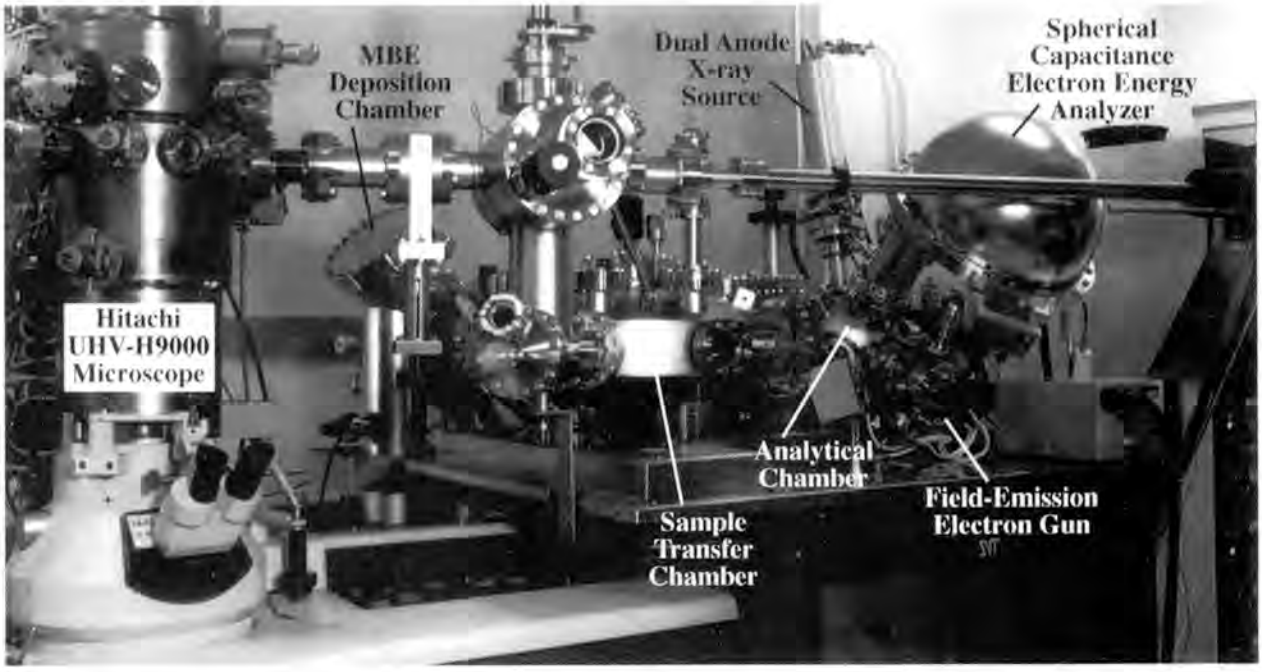

Figure 1. Photograph of the Hitachi UHV H-9000 microscope attached to the Sample Preparation Evaluation Analysis and Reaction (SPEAR) system.

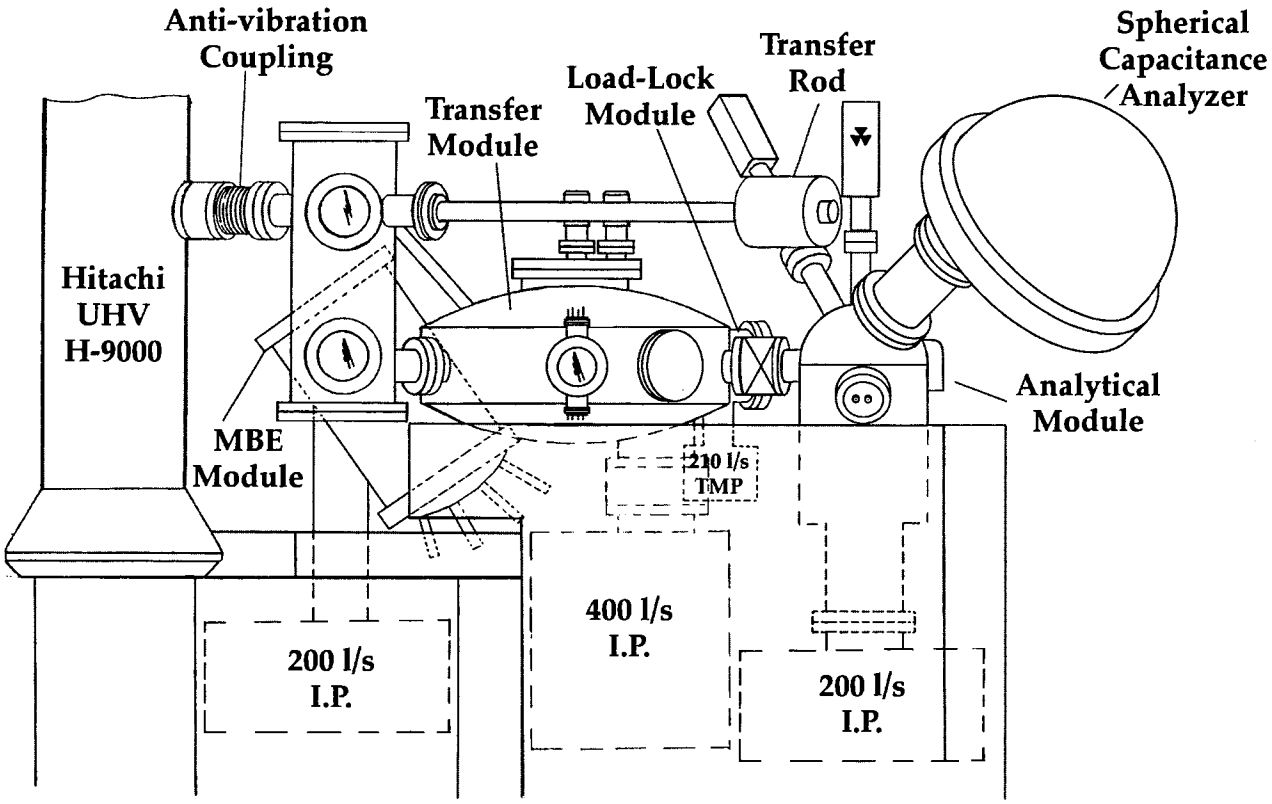

Figure 2. Schematic of the surface analysis system.

cells, and it is currently configured for thin film deposition of GaAs. The sample stage heats specimens resistively during deposition for epitaxial thin film growth.

The dual role of the analytical chamber is to prepare and chemically characterize surfaces. Samples are cleaned through a combination of sequential ion milling and annealing. The chemical properties of the specimen surface are then studied through the use of XPS and AES. The analytical chamber is also fitted with a heating/cooling stage for temperature control during preparation and analysis.

Ion milling is accomplished using a duoplasmatron ion source with a microbeam ion gun column (Physical Electronics). The gun has a variable gas source and can produce oxygen, argon, or xenon ions with a minimum probe size of <5 μm. The maximum accelerating voltage is 10 kV and is operable down to a minimum voltage of 250 V. The configuration of the sample stage also allows the sample to be floated at a positive or negative DC bias, allowing the ion gun to operate at a more usable accelerating voltage without inducing undesired damage to the sample surface. The duoplasmatron ion gun produces a maximum current density of 20 mA/cm^2 for a 50-μm beam diameter. Using a Channeltron (channel electron multiplier) detector and a video imaging system, ion-induced secondary electron images can be acquired during milling, providing precise control over the location being milled.

Two different methods of annealing are available in the analytical chamber. The first is a resistive heating method similar to the one present in the MBE chamber. Samples may be heated in excess of 1000°C, depending on the quality of the contact between the sample and its holder. The second method of annealing is through the use of a 1- to 10-keV electron gun (Kimball Physics Inc., Wilton, NH) that is capable of heating the sample to 2000°C. The specimen may also be cooled using a liquid nitrogen cooled cold finger that is brought into contact with the sample stage.

Chemical analysis is accomplished using a spherical capacitance electron energy analyzer (SCA) (Physical Electronics). It has an energy resolution of 0.1 eV and is capable of detecting changes in chemical states due to bonding at the surface. The analyzer also has an electrostatic lens that can define an analysis area of 10 mm × 3 mm down to 70μm × 70μm. A dual-anode X-ray source (Physical Electronics), capable of producing either Al Kα or Mg Kα X-rays with a maximum output power of 400 W per anode, is used for acquisition of XPS spectra.

The analytical chamber also contains a single-lens electron focusing column with scanning capabilities (FEI Co., Hillsboro, OR), including an asymmetric electrostatic lens (Orloff and Swanson, 1979) and a thermal field emitter or "Schottky" emitter (SE) (Tuggle and Swanson, 1985). When combined with the SCA, AES spectra (Tuggle et al., 1979) can be acquired with a high spatial resolution.

SEM images can also be obtained with a 15-kV electron beam and a 50-nm probe size.

3. Preliminary Results (*Illustrating Capabilities*)

We describe here, briefly, some preliminary data from examining conventional transmission electron microscope samples using surface science techniques. All TEM samples were prepared *ex situ* using standard mechanical polishing and chemical etch techniques (Booker and Stickler, 1962; Xu et al., 1993).

To roughly determine the detection limit of the SCA, a test sample was prepared using a 1000 mesh gold grid dusted with zirconia powder containing 7 wt% Cu. The approximate surface area coverage was estimated using SEM to be between 10 and 15%. Figure 3a is the XPS spectrum of the sample, illustrating the various chemicals detected. Peaks corresponding to oxygen, carbon, gold from the grid, zirconium, and copper can be seen. The copper peak is highlighted in Figure 3b.

For purposes of calibrating the AES, analysis was done on the surface of a GaAs(100) bulk sample. The sample was heated to excess, producing Ga islands on the surface of the sample. SEM was used to identify and measure the dimensions of the islands, illustrated in Figure 4. The chemical composition of these islands relative to the surrounding surface were then characterized using AES. Figure 5 shows the spectra acquired from the two different regions of the sample. From the data it is evident that during heating, arsenic desorbed from the surface leaving gallium-rich islands behind.

The silicon system has been studied using the SSC side chamber system (Dunn et al., 1991; Marks et al., 1993; Jayaram et al., 1993; Plass and Marks, 1995),

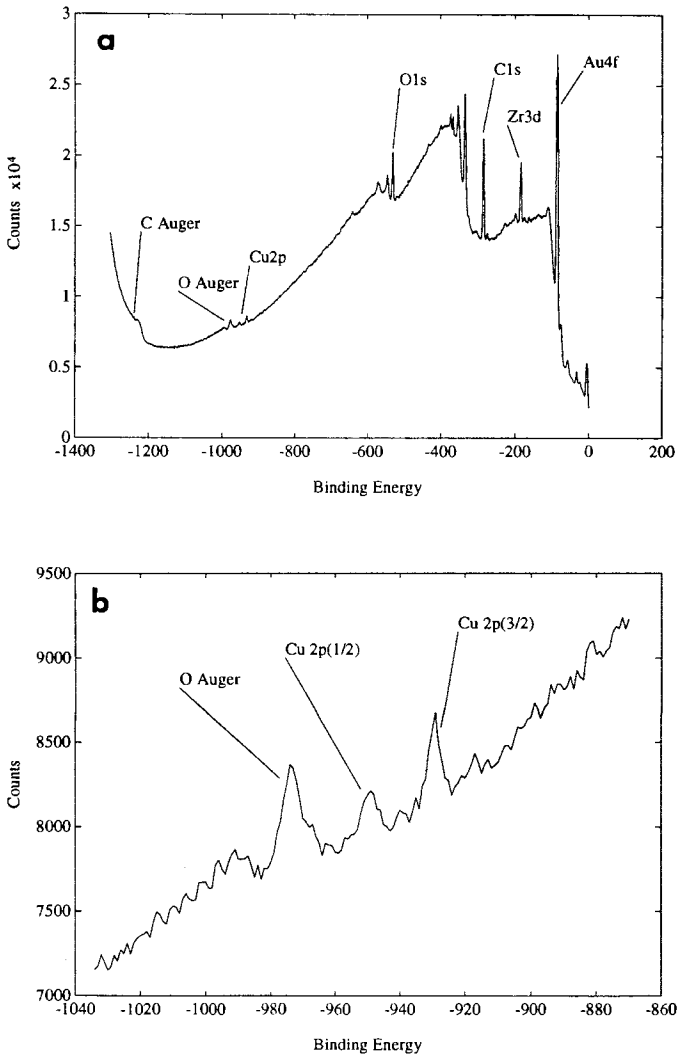

Figure 3. XPS spectra from Zirconia powder with 7 wt.% copper dispersed on gold grid. Photoelectrons were produced using aluminum Kα radiation. (a) Scan over the full binding energy range. (b) Blow-up of Cu2p region.

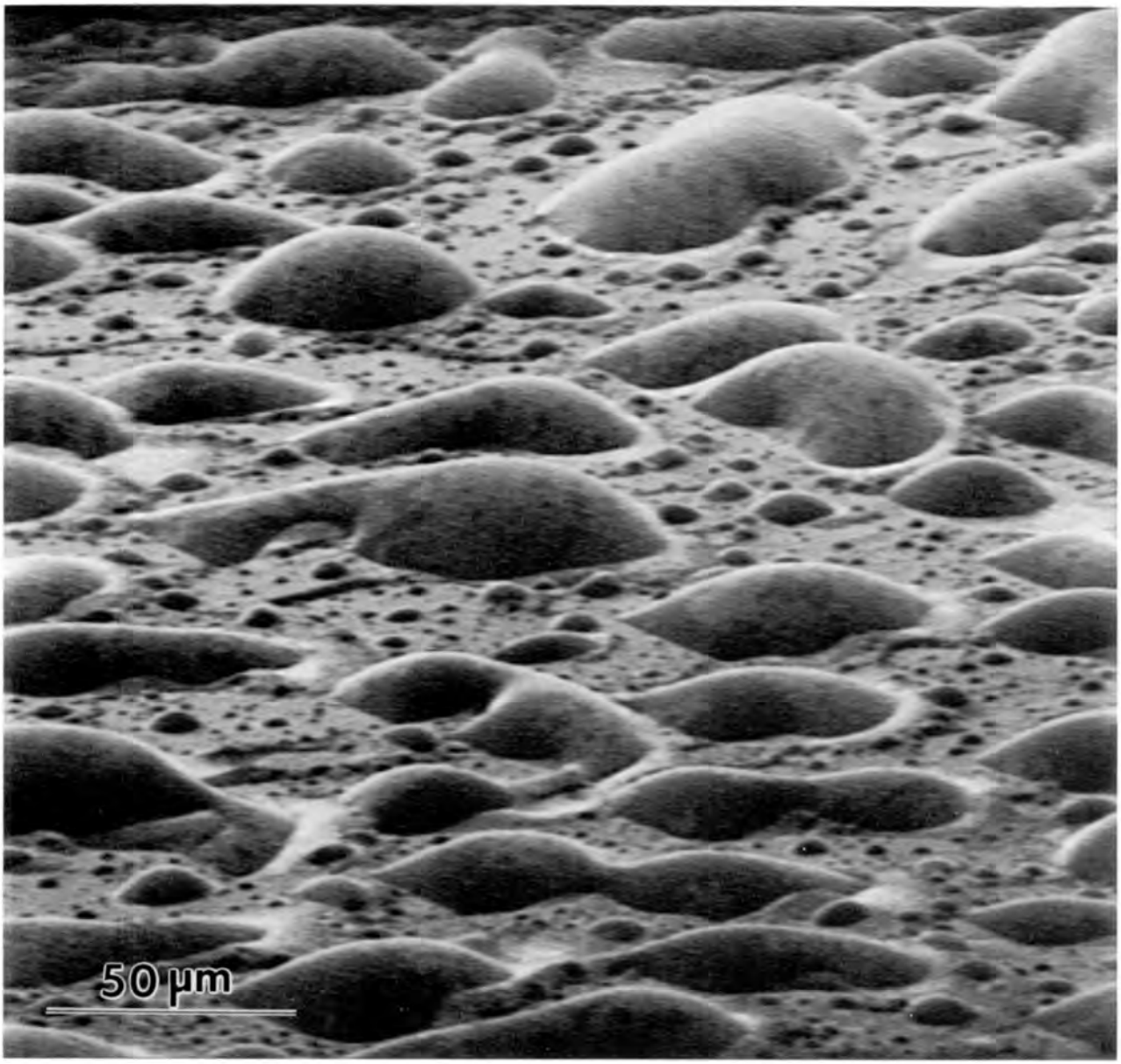

Figure 4. SEM image of Ga islands on a GaAs substrate.

making it a useful standard for comparing the abilities of SPEAR to that of its predecessor. The as-etched silicon samples were characterized using XPS, Figure 6a. Ion milling with 4-kV oxygen ions for 6 min on each side was sufficient to remove all carbon contamination from the surface, Figure 6b. Afterward, it was annealed using the Kimball Physics high-current electron gun to a temperature of 750°C for 5 min. After a brief inspection in the microscope, it was returned to the analytical chamber and milled with 3-kV argon ions at 30 degrees from the surface for 5 min on one side to obtain thin regions. It was then annealed again at 630°C for 2 min. When the sample was returned to the microscope, the Si(001)-2 × 1 reconstruction could be identified, Figure 7.

Using the Channeltron detector and the video imaging system, ion-induced secondary electron images were acquired during milling, providing very precise control over the milled region. Figure 8a is an ion beam-induced image of a Si(111) sample just after 5 min of milling using a 1.5-kV oxygen ion beam. Following a second ion milling of the surface for 8 min using a 1.5-kV beam of argon

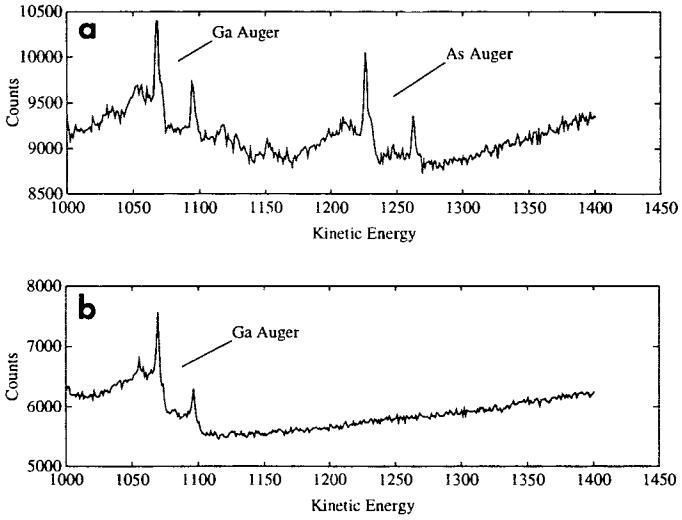

Figure 5. Auger spectra from the surface shown in Figure 4. (a) Spectrum from area between islands showing both Ga and As signals. (b) Spectrum from an island showing Ga and no As.

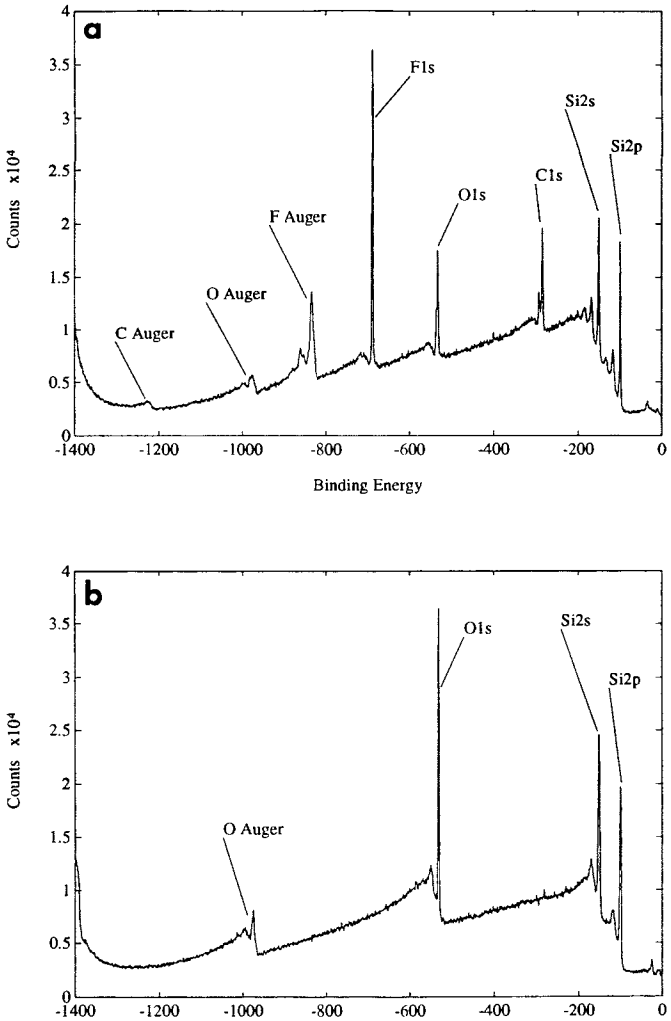

Figure 6. XPS spectra from Si(001) sample. (a) The as-etched surface. (b) After a 6-min ion mill using 4-kV oxygen ions.

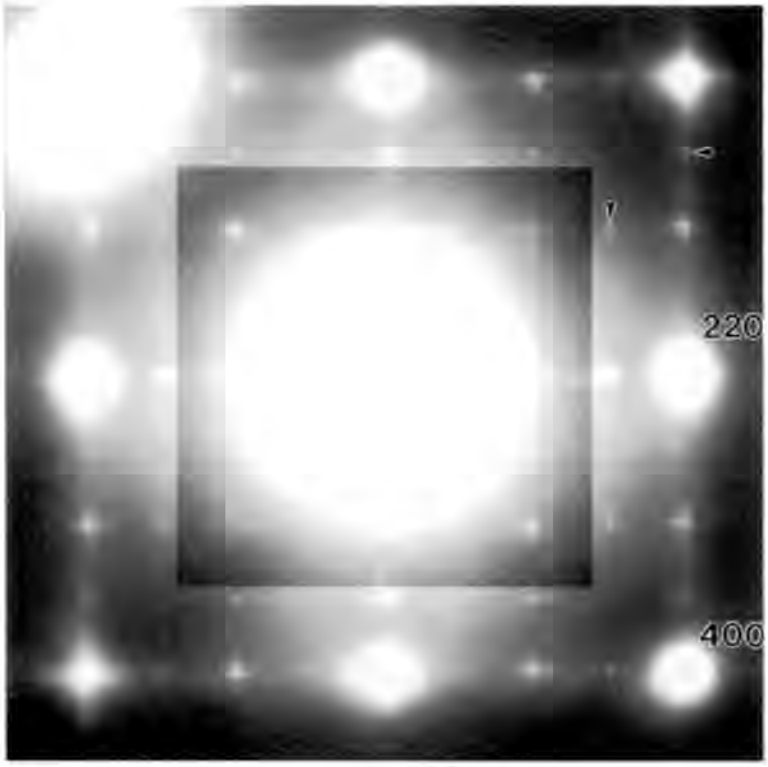

Figure 7. Transmission electron diffraction pattern from a Si(001) sample showing two domains of the 2×1 surface reconstruction. Arrows indicate two surface spots.

ions, there is a sharp contrast in the image between the previous region milled using an oxygen ion beam and the second region, Figure 8b.

Germanium (001) samples were cut from a wafer, dimpled, and chemically etched using the same etching technique as for silicon, inserted into the system, and characterized as-etched using XPS, Figure 9a. The sample was initially milled at 4 kV with oxygen ions at 60 degrees from the surface for 6 min per side to remove carbon contamination, shown in Figure 9b, and then annealed using the Kimball Physics electron gun at 400°C for 4 min to desorb the oxygen. A second ion mill of 3-kV argon ions 30 degrees from the surface on one side was performed to thin the sample that was then annealed at 400°C for 4 min. This resulted in a 2×1 surface reconstruction seen in the TED pattern, Figure 10. Further milling and annealing steps were then used to strengthen the surface reconstruction.

4. Discussion

The results described herein indicate that the SPEAR system is reaching its expectations for preparing surfaces *in situ* and chemically characterizing them. Consequently, any future work will have the tools available to correlate a given surface structure with surface chemical information. While the improvements over the previous SSC are extensive, the SPEAR system has its own limitations that will have to be dealt with in realizing its full potential for surface studies. The approach of placing all of the sample preparation and characterization equipment in different chambers allows a large number of techniques to be integrated into the same system; however, it also necessitates frequent sample transfers for each experiment. Moving samples around presents two problems. First, the sample stages in the analysis and MBE chambers are designed to pick up a sample from the transfer rod and rely only on spring tension to hold the specimen. The sample holders have no "bottoms" to keep gravity from pulling a sample out, and occasionally during heating or transfer an improperly gripped sample will fall. While experience with the system has made the dropping of a sample a rare event, the loss of a well-prepared and characterized TEM sample can translate into a significant loss of time. The second drawback of transfer stems from the inherent fragility of an electron-

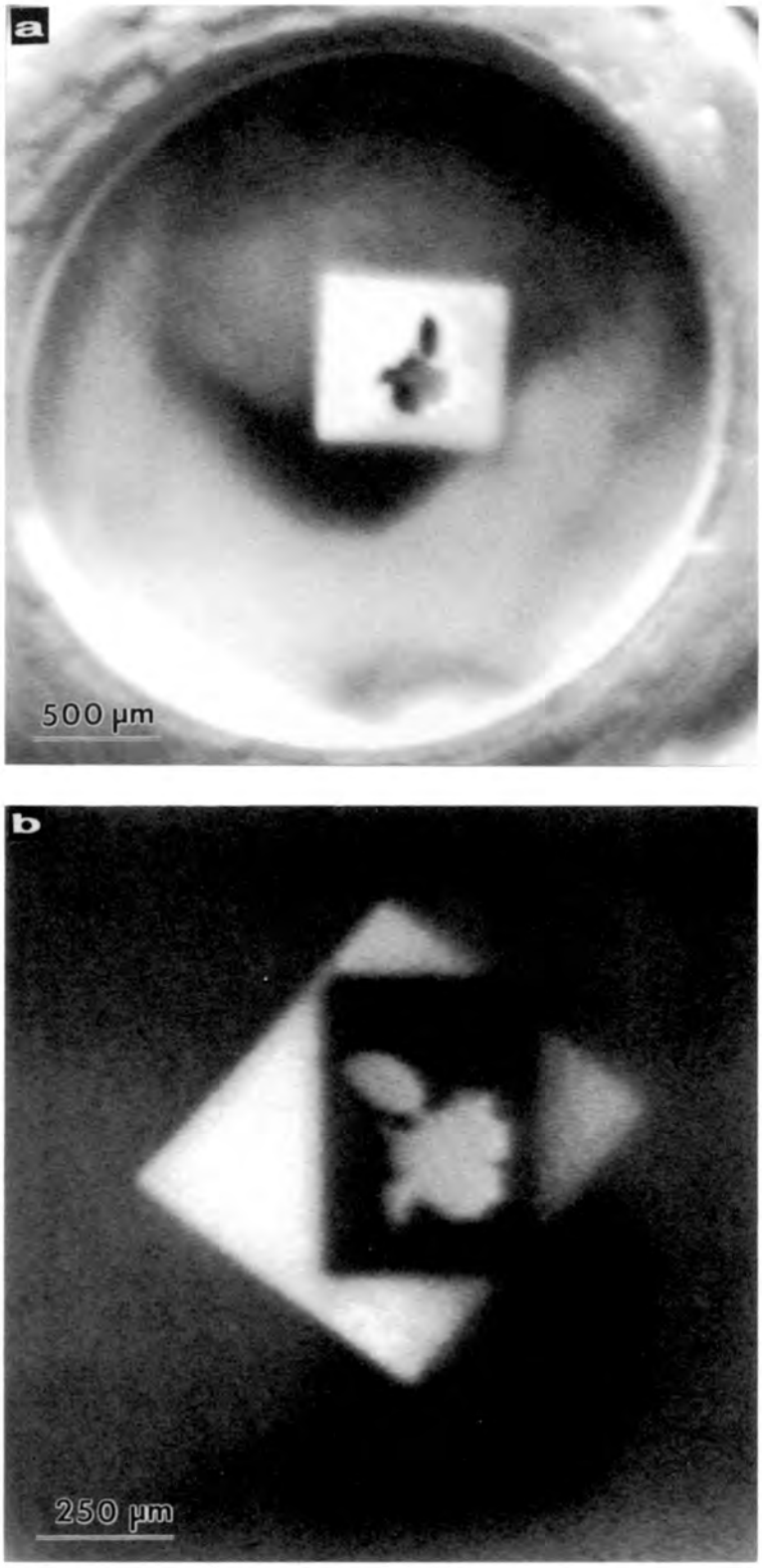

Figure 8. Ion beam-induced secondary electron images of a Si(111) sample. (a) 1.5-kV oxygen beam image taken after a 6-min mill. The bright square is the milled region. The irregularly shaped dark area in the middle of the milled region is a hole in the sample. (b) 1.5-kV argon beam image taken after an 8-min mill. The beam raster was rotated 45 degrees with respect to the previous oxygen mill creating the dark rectangle within the lighter square.

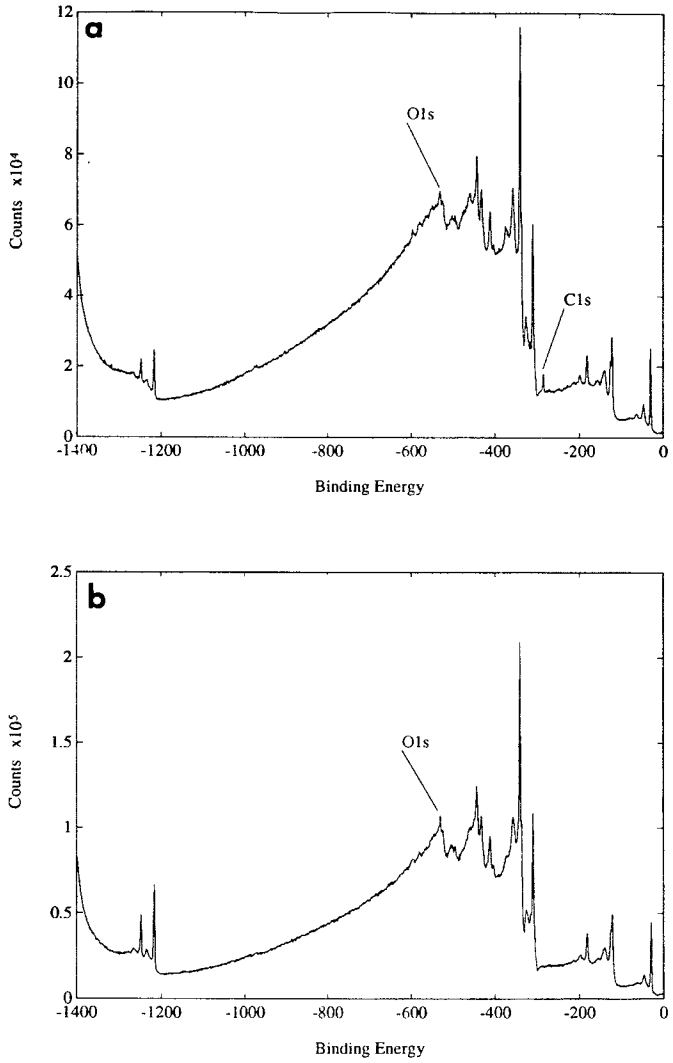

Figure 9. XPS spectra from Ge(001) sample. Oxygen 1 s and carbon 1 s peaks are labeled. All other peaks correspond to germanium core level and Auger lines. (a) The as-etched surface. (b) After a 6-min ion mill using 4-kV oxygen ions.

transparent sample. Although the transfer system is well designed and operates smoothly, small vibrations during a sample transfer have proven dangerous to delicate materials. While silicon and germanium are sufficiently robust, we have seen the thin regions of several GaAs samples fracture during transfer.

One of SPEAR's strengths is also another one of its limitations. With the large amount of sophisticated equipment, a correspondingly larger number of maintenance delays should be expected. In order to minimize this problem, the system has been designed so that each of the three main chambers and the microscope can be brought up to air and pumped back down independently of all others. Also, each individual experiment is unlikely to require the use of all the available equipment, and flexibility in planning different studies can maximize the operating time of the system as a whole. However, maintenance of the equipment is still a concern, and only time will reveal how much of a challenge it presents.

Acknowledgments

We would like to acknowledge the support of the National Science Foundation on grants #DMR-9204117 and #DMR-9214505, and the support of the Air Force Office of Scientific Research on grants #F49620-94-1-0164 and #F49620-92-J-0250 in funding this work.

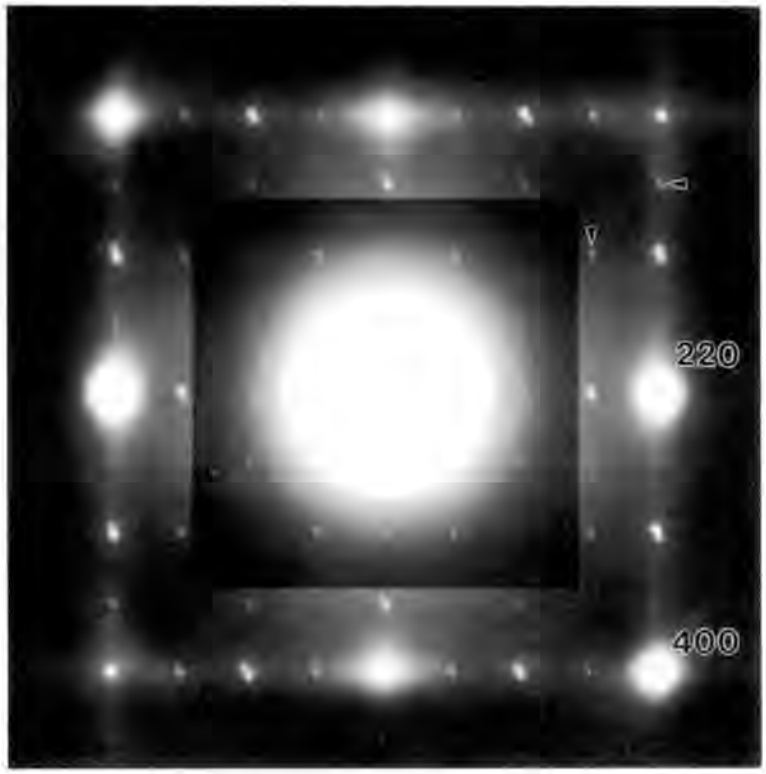

Figure 10. Transmission electron diffraction pattern from a Ge(001) sample showing two domains of the 2×1 surface reconstruction. Arrows indicate two surface spots.

References

Bauer, E., Mundschau, M., Swiech, W., and Telieps, W. (1989) Surface studies by low-energy electron microscopy (LEEM) and conventional UV photoemission electron microscopy (PEEM), *Ultramicroscopy*, 31, 49–57.

Bleeker, A.J. (1991) A UHV scanning transmission electron microscope for Auger electron spectroscopy, Ph. D. Dissertation, Delft TU.

Bonevich, J.E. and Marks, L.D. (1992) Ultrahigh vacuum electron microscopy of crystalline surfaces, *Microscopy: The Key Research Tool*, 22(1), 95–102.

Booker, G.R. and Stickler, R. (1962) Method of preparing Si and Ge specimens for examination by transmission electron microscopy, *Brit. J. Appl. Phys.*,13, 446–448.

Briggs, D. and Seah, M.P. (1983) *Practical surface analysis: by Auger and X-ray photoelectron spectroscopy*, John Wiley and Sons, New York.

Cherns, D. (1974) Direct resolution of surface atomic steps by transmission electron microscopy, *Phil. Mag.*, 30, 549–556.

Dunn, D.N., Ai, R., Savage, T.S., Zhang, J.P., and Marks, L.D. (1991) Preparation and detection of reconstructed plan-view surfaces, *Ultramicroscopy*, 38, 333–342.

Endo, A. and Ino, S. (1993) Observation of the Ag/Si(111) system using a high-resolution ultrahigh vacuum scanning electron microscope, *Surf. Sci.*, 293, 165–182.

Gibson, J.M. (1990) Evidence for a stable Si(111)7×7 : 0 reconstruction from quantitative transmission electron diffraction, *Surf. Sci.*, 239, L531– L536.

Griffith, O.H. and Engel, W. (1991) Historical perspective and current trends in emission microscopy, mirror electron microscopy, and low-energy electron microscopy, *Ultramicroscopy*, 36, 1–28.

Heinemann, K. and Poppa, H. (1986) An ultrahigh vacuum multipurpose specimen chamber with sample introduction system for *in situ* transmission electron microscopy investigations, *J. Vac. Sci. Tech.*, A4(1), 127–136.

Hembree, G.G., Crozier, P.A., Drucker, J.S., Kishnamurthy, M., Venables, J.A., and Cowley, J.M. (1989) Biased secondary electron imaging in a UHV-STEM, *Ultramicroscopy*, 31, 111–115.

Honjo, G., Takayanagi, K., Kobayashi, K., and Yagi, K. (1977) Ultra-high vacuum *in situ* electron microscopy of growth processes of epitaxial thin films, *J. Crys. Growth*, 42, 98-109.

Jayaram, G., Plass, R., and Marks, L.D. (1995) UHV-HREM and diffraction of surfaces, *Interface Sci.*, 2, 379–395.

Jayaram, G., Xu, P., and Marks, L.D. (1993) Structure of Si(100)-(2×1) surface using UHV transmission electron diffraction, *Phys. Rev. Lett.*, 71, 3489–3492.

Kondo, Y., Ohi, K., Ishibashi, Y., Hirano, H., Harada, Y., Takayanagi, K., Tanishiro, Y., Kobayashi, K., and Yagi, K. (1991) Design and development of an ultrahigh vacuum high-resolution transmission electron microscope, *Ultramicroscopy*, 35, 111–118.

Kondo, Y., Ohi, K., Ishibashi, Y., Hirano, H., Kobayashi, H., Harada, Y., Takayanagi, K., Tanishiro, Y., Kobayashi, K., Yamamoto, N., and Yagi, K. (1987) Development of ultra-high vacuum transmission electron microscope. II. Vacuum system, *J. Electron Micros.*, 36, 227–338.

LaFemina, J.P. (1992) Total-energy calculations of semiconductor surface reconstructions, *Surface Science Reports*, 16, 138–248.

Marks, L.D. (1983) Direct imaging of carbon-covered and clean gold (110) surfaces, *Phys. Rev. Lett.*, 51, 1000–1002.

Marks, L.D., Ai, R., Bonevich, J.E., Buckett, M.I., Dunn, D., Zhang, J.P., Jacoby, M., and Stair, P.C. (1991) UHV microscopy of surfaces, *Ultramicroscopy*, 37, 90–102.

Marks, L.D., Ai, R., Savage, S., and Zhang, J.P. (1993) Ultrahigh vacuum microscopy of the Si(111) boron $\sqrt{3} \times \sqrt{3}$ R30° surface, *J. Vac. Sci. Technol.*, A11(3), 469–473.

Marks, L.D., Kubozoe, M., Tomita, M., Ukiana, M., Furutsu, T., and Matsui, I. (7 – 12 August 1988, Milwaukee, WI) Design and initial performance of a UHV-HREM: pp. 658–659 in *Instrumentation and Computer Applications*, Proc. 46th EMSA, ed. by G.W. Bailey, pub. by San Francisco Press, San Francisco.

Marks, L.D., Xu, P., Dunn, D.N., and Zhang, J.P. (1992) Atomic imaging of surfaces in plan view, *EMSA Bull.*, 22, 65–69.

Métois, J.J., Nitsche, S., and Heyraud, J.C. (1989) An ultrahigh-vacuum transmission and scanning electron microscope for crystal growth experiments, *Ultramicroscopy*, 27, 349–358.

Milne, R.H., Hembree, G.G., Drucker, J.S., Harland, C.J., and Venables, J.A. (1993) Surface studies in UHV SEM and STEM, *J. Micros.*, 170(3), 193–199.

Mundschau, M. (1991) Emission microscopy and surface science, *Ultramicroscopy*, 36, 29–51.

McCartney, M.R. and Smith, D.J. (1991) Studies of electron irradiation and annealing effects on TiO_2 surfaces in ultrahigh vacuum high-resolution electron microscopy, *Surf. Sci.*, 250, 169–178.

McDonald, M.L. and Gibson, J.M. (1984) An ultrahigh vacuum and ultrahigh resolution transmission electron microscope, pp. 436–437, Proc. 42nd EMSA, ed. by G.W. Bailey, pub. by San Francisco Press, San Francisco.

Nielsen, P.E.H. and Cowley, J.M. (1976) Surface imaging using diffracted electrons, *Surf. Sci.*, 54, 340–354.

Orloff, J. and Swanson, L.W. (1979) An asymmetric electrostatic lens for field-emission microprobe applications, *J. Appl. Phys.*, 50(4), 2494–2501.

Plass, R. and Marks, L.D. (1995) UHV transmission electron microscopy structure determination of the Si(111)-($\sqrt{3} \times \sqrt{3}$)R30° Au Surface, *Surf. Sci.*, 342, 233–249.

Rohrer, H. (1994) Scanning tunneling microscopy: a surface science tool and beyond, Surf. Sci., 299/300, 956–964.

Siegbahn, K., Nordling C., Fahlman, A., Nordberg, R., Hamrin, K., Hedman, J., Johannson, G., Belgmark, T., Karlsson, S.E., Lindgren, I., and Lindberg, B. (1967) *ESCA — Atomic, Molecular, and Solid State Structure Studied by Means of Electron Spectroscopy*, Almfquist & Wiksell, Uppsala.

Smith, D.J., Podbrdsky, J.J., Swann, P.R., and Jones, J.S. (1989) Initial experiences with a 300 kV HREM converted for UHV operation, *Mater. Res. Symp. Proc.*, 139, 282–294.

Takayanagi, K., Tanishiro, Y., Takahashi, S., and Takahashi, M. (1985) Structure analysis of Si(111)- 7×7 reconstructed surface by transmission electron diffraction, *Surf. Sci.*, 164, 367–392.

Tromp, R.M. and Reuter, M.C. (1993) Imaging with a low-energy electron microscope, *Ultramicroscopy*, 50, 171–178.

Tromp, R.M. (1994) Low-energy electron microscope, *MRS Bull.*, 6, 44–46.

Tuggle, D.W. and Swanson, L.W. (1985) Emission characteristics of the ZrO/W thermal field electron source, *J. Vac. Sci. Technol. B*, 3(1), 220–223.

Tuggle, D.W., Swanson, L.W., and Orloff, J. (1979) Application of a thermal field-emission source for high resolution, high current e-beam microprobes, *J. Vac. Sci. Technol.*, 16(6), 1699–1703.

Twesten, R.D., Gibson, J.M., and Ross, F.M. (1994) Visualization of dynamic near-surface processes, *MRS Bull.*, 6, 38–43.

Venables, J.A., Smith, D.J., and Cowley, J.M. (1987) HREM, STEM, REM, SEM and STM, *Surf. Sci.*, 181, 235–249.

Wilson, R.J. and Petroff, P.M. (1983) Cryopump and sample holder for clean reconstructed surface observations in a transmission electron microscope, *Rev. Sci. Instrum.*, 54(1), 1534–1537.

Xu, H., Hashizume, T., and Sakurai, T. (1993) GaAs(100) (2×4) surface study by molecular beam epitaxy and field-ion-scanning-tunneling-microscopy, *Jpn. J. Appl. Phys.*, 32(3B), 1511–1514.

Yagi, K. (1993) Reflection electron microscopy: studies of surface structure and surface dynamic processes, *Surface Science Reports*, 17, 305–362.